Submitted to JGR, December 26, 1998

Subsidence, Mixing and Denitrification of Arctic Polar Vortex Air Measured During POLARIS

M. Rex[1], R. J. Salawitch[1], G. C. Toon[1], B. Sen[1], J. J. Margitan[1], G. B. Osterman[1], J.-F. Blavier[1], R. S. Gao[2], S. Donnelly[2], E. Keim[2], J. Neuman[2], D. W. Fahey[2], C. R. Webster[1], D. C. Scott[1], R. L. Herman[1], R. P. May[1], E. J. Moyer[1], M. R. Gunson[1], F. W. Irion[1], A. Y. Chang[1], C. P. Rinsland[3], and T. P. Bui[4].

Abstract. A new technique is presented to determine the degree of denitrification that occured during the 1996/97 Arctic winter, based on balloon and aircraft borne measurements of NO_y, N_2O and CH_4. The NO_y / N_2O relation can undergo significant change due to isentropic mixing of subsided vortex air masses with extra-vortex air due to the high non-linearity of the relation. In this study high-altitude balloon measurements are used to define the properties of air masses that later descend in the polar vortex to altitudes sampled by the ER-2 aircraft (i.e. 20km) and mix isentropically with mid-latitude air. Observed correlations of CH_4 and N_2O obtained are used to quantify the degree of subsidence and mixing for individual air masses. Based on these results the expected mixing ratio of NO_y resulting from subsidence and mixing, defined here as NO_y**, is calculated and compared with the measured mixing ratio of NO_y. NO_y and NO_y** agree well during most parts of the flights. A slight deficit of NO_y vs. NO_y** is found only for a limited region during the ER-2 flight on April 26, 1997. This deficit is interpreted as indication for weak denitrification (~2-3 ppbv) in that air mass. The small degree of denitrification is consistent with the temperature history of the sampled air, which hardly encountered temperatures below the frostpoint during the Arctic winter 1996/97. Much larger degrees of denitrification would have been inferred if mixing effects had been ignored, which is the traditional approach to diagnose denitrification. Our analysis demonstrates the importance of using other correlations of conserved species to be able to accurately interpret changes in the NO_y / N_2O relation with respect to denitrification.

1. Introduction

Rapid loss of ozone in the Arctic vortex during winter and spring is caused by catalytic cycles driven by active chlorine species (ClO_x = Cl, ClO, Cl_2O_2) (e.g. Salawitch et al., 1990; Waters et al., 1993). Elevated levels of ClO_x result from heterogenous reactions of HCl and $ClONO_3$ on polar stratospheric cloud (PSC) particles, which form at low temperatures during winter in the Arctic region (e.g. Brune et al., 1990; Webster et al., 1993; Notholt et al., 1995). Following the evaporation of PSCs, the lifetime of elevated ClO_x and hence the time period of rapid ozone

[1]Jet Propulsion Laboratory, California Institute of Technology, Pasadena, California, USA
[2]Aeronomy Laboratory, National Oceanic and Atmospheric Administration, Boulder, Colorado, USA
[3]Langley Research Center, National Aeronautics and Space Administration, Hampton, Virginia, USA
[4]Ames Research Center, National Aeronautics and Space Administration, Moffett Field, California, USA

loss is mainly controlled by the amount of NO_2 in the vortex (e.g. Brune et al., 1991; Salawitch et al., 1993). Levels of NO_2 are quite small during the Arctic winter due to heterogeneous conversion of NO_x (NO, NO_2) to HNO_3 (e.g. Kawa et al., 1992). In spring, the production rate of NO_2 from the photolysis of HNO_3 rises due to the increase in the intensity of solar UV-irradiance in the lower stratosphere. The released NO_2 reacts rapidly with ClO to form the passive reservoir species $ClONO_2$ (e.g. Toon et al., 1992; Roche et al., 1994). This mechanism effectively slows down the Arctic ozone loss rate in spring and limits the overall loss of ozone in the Arctic vortex (e.g. Brune et al., 1991; Salawitch et al., 1993).

Denitrification, the permanent removal of NO_y (total reactive nitrogen) by the sedimentation of HNO_3-bearing PSC particles, can lead to a reduced production of NO_2 during spring (Toon et al., 1986). Widespread severe denitrification is common in the Antarctic (e.g. Toon et al., 1989, Fahey et al., 1990, Santee et al., 1995). Patches of denitrified air have also been observed in the Arctic after exceptionally cold Arctic winters (e.g. Fahey et al, 1990; Huebler et al., 1990; Arnold et al., 1996; Oelhaf et al., 1996, Hintsa et al., 1998). For the Arctic winter of 1995/96, the coldest Arctic winter on record, the period of ozone loss was prolonged due to denitrification and the overall ozone loss reached record values in the layer of air that experienced the longest period of cold conditions favourable for denitrification (Rex et al., 1997).

The degree of denitrification in a given air mass has been typically estimated by comparison of measured mixing ratios of NO_y with the expected abundance of NO_y (defined as NO_y*) calculated from simultaneous observations of N_2O and well established correlations between the mixing ratios of NO_y and N_2O (e.g., Toon et al., 1989, Fahey et al., 1990; Rinsland et al., 1998). This method is based on the assumption that the mixing ratios of two long lived tracers (i.e., chemical lifetime long compared to mixing lifetime) develop a compact relationship independent of altitude and latitude (Plumb and Ko, 1992). Severe denitrification is common throughout the Antarctic vortex and can be inferred in a straightforward manner by examination of the NO_y versus N_2O relation (e.g., Fahey et al., 1990).

In contrast to the picture of well preserved tracer / tracer relationships which can be changed only by chemistry or denitrification, Waugh et al. (1997), Kondo et al. (1998) and Michelsen et al. (1998) have recently proposed that isentropic mixing of subsided inner-vortex with extra-vortex air masses can lead to substantial changes in the NO_y / N_2O relationship without denitrification. Kondo et al. (1998) and Michelsen et al. (1998) have also suggested that dynamically induced changes in the NO_y / N_2O correlation can be mistaken for denitrification. The NO_y versus N_2O relation is highly non-linear, making it particularly sensitive to changes induced by descent and mixing (discussed in more detail below). Dessler et al. (1998) have noted more generally that the unique tracer / tracer relationships in the Plumb and Ko (1992) framework are not preserved under the special conditions of the polar vortices where redistribution of tracers by vertical transport is comparably fast to isentropic (quasi-horizontal) mixing. Waugh et al. (1997) showed examples of a change in the relationship of several pairs of long-lived tracers that was connected with mixing processes in the vicinity of the polar vortex. In the Arctic vortex, severe denitrification is rare (e.g. Santee et al., 1995, Rinsland et al., 1998), and changes in the NO_y / N_2O relationship caused by descent and isentropic mixing can easily mask changes caused by moderate denitrification.

The focus of our paper is the development of a technique to account for changes in the NO_y / N_2O relationship due to descent and isentropic mixing so that the degree of denitrification can be accurately quantified. The tracer / tracer relationship of a pair of long-lived tracers that does not include NO_y is first examined to quantify the dynamically induced changes that affect the measured airmasses. The selected pair of tracers should have a long chemical lifetime in the stratosphere. Dynamically induced changes can only be quantified if the tracer/tracer relationship prior to isentropic mixing are non-linear. We therefore use the CH_4 / N_2O relationship to quantify descent and mixing because the extra-vortex correlation is non-linear (Herman et al., 1998; Michelsen et al., 1998), both gases are long-lived (lifetimes longer than 1 year at 30 km increasing to longer than 50 years at 20 km), and measurements of both gases have been obtained by instruments onboard the ER-2 as well as by the balloon-borne MkIV and ALIAS II instruments at high latitude during POLARIS. Previously, Michelsen et al. (1998) and Herman et al. (1998) have shown that isentropic mixing in the vicinity of the Arctic vortex tends to reduce the non-linearity of the CH_4 / N_2O correlation.

2. Data sets

In this work, we utilize observations obtained by instruments aboard the NASA ER-2 aircraft and several balloon borne instruments during the POLARIS mission. Instruments aboard the ER-2 provided in-situ measurements of many important stratospheric gases for a wide range of latitudes and altitudes near 20 km. During POLARIS, balloon-borne instruments complemented the ER-2 measurements by providing vertical profiles of stratospheric gas concentrations using both in-situ and remote sensing techniques.

Measurements aboard the ER-2 of N_2O and CH_4 were made by ALIAS (Aircraft Laser Infrared Absorption Spectrometer). ALIAS is a scanning tunable diode laser spectrometer that measures CH_4, N_2O, HCl and CO using high resolution laser absorption in the 3-8 μm wavelength region [Webster et al., 1994]. ALIAS II provided in situ measurements of CH_4 and N_2O from the Observations from the Middle Stratosphere (OMS) in-situ balloon gondola. The OMS suite of instruments flew during the POLARIS campaign on June 30, 1997. ALIAS and ALIAS II measure N_2O and CH_4 with an estimated 5% accuracy, and precisions of 1% and 5%, respectively [Herman et al., 1998]. ER-2 measurements of NO_y were made by the NOAA Aeronomy Laboratory reactive nitrogen instrument. The instrument measures total nitrogen by catalytically reducing NO_y to NO, then detecting NO through chemiluminescent reaction with O_3. NO_y is measured with a total 1 σ uncertainty of less than 10% [Fahey et al., 1989]. Here we examine ER-2 observations obtained on the two poleward flights from Fairbanks, Alaska (65°N, 148°W) that encountered polar vortex air (April 26 and June 30, 1997) and the OMS observations obtained on June 30, 1997 near Fairbanks.

The MkIV Fourier Transform Infra-Red (FTIR) spectrometer [Toon, 1991] obtains remote measurements of the composition of the atmosphere using the solar occultation technique. The brightness and stability of the Sun allow high signal-to-noise ratio spectra with broad coverage (650-5650 cm^{-1}) to be obtained at high spectral resolution (0.01 cm^{-1}), allowing the abundances of a large number of gases to be measured simultaneously. The retrieval algorithm, spectroscopic parameters and measurement uncertainties are discussed by Sen et al. [1996, 1998]. Gases measured by MkIV relevant to this work include O_3, N_2O and CH_4. It also provides a complete

determination of NO_y by measuring NO, NO_2, HNO_3, HNO_4, N_2O_5 and $ClNO_3$. The measurement of CH_4 and N_2O have an accuracy and precision of 5%. The precision of NO_y for 20 km is ~5% with an accuracy of 15%. Here we examine data obtained by the MkIV instrument on the May 8, 1997 balloon flight near Fairbanks.

3. Data analysis and results

3.1. NO_y / N_2O relationship

Figure 1 shows the NO_y / N_2O relationship measured at high latitude during POLARIS by the MkIV infrared spectrometer between 8 and 37 km on May 8, 1997 and by the NO_y and ALIAS instruments on board the ER-2 on an isentropic level (500-510 K) near 20km on April 26, 1997. Potential vorticity analyses and the relation between N_2O and potential temperature (e.g. N_2O= 200 ppbv at 500K: typical values of N_2O inside the vortex at 500K are much lower) indicate that the MkIV profile was obtained outside of the polar vortex. In Figure 2 we compare the MkIV measurements to other (non-POLARIS) ER-2 NO_y / N_2O measurements (Loewenstein et al., 1993) to demonstrate that the differences here (Figure 1) are not platform or instrument related. The MkIV measurements of NO_y and N_2O are similar to the well established reference relationship between these tracers at mid-latitudes (Chang et al., 1996; Sen et al., 1998; Keim et al., 1997 - black lines in Figure 2) and agree well with earlier measurements obtained by ER-2 instruments at similar latitudes during the Arctic winter (e.g. the flight on January 3, 1989, green points in Figure 2). For mixing ratios of N_2O below ~100 ppbv, the relation between NO_y / N_2O is highly non-linear and exhibits a peak near 30 km due to rapid loss of NO_y at high altitudes due to the reaction N+NO (e.g. Russell et al., 1988; Nevison et al., 1997). The NO_y / N_2O relationship measured by MkIV (Figure 1) is used in this work to represent the conditions in the vortex prior to denitrification, descent, and isentropic mixing. Compared with this reference relation, severe NO_y deficits were observed in the Arctic during a number of ER-2 flights in February 1989 (e.g. the flights on February 7, 1989, magenta points in Figure 2). In contrast, the ER-2 observations obtained inside the Arctic vortex on April 26, 1997 during POLARIS show only moderate deficits of NO_y compared to the reference NO_y / N_2O relationship for air with mixing ratios of N_2O below ~200 ppbv (Figure 1).

The moderate deficit of NO_y observed during POLARIS could be due to one of several processes: (1) denitrification, (2) descent followed by isentropic mixing, and (3) a combination of (1) and (2). Denitrification (process (1)) is illustrated by the dot-dashed arrow in Figure 1: starting from the MkIV NO_y / N_2O reference correlation, this process could have reduced the NO_y mixing ratio without changing the N_2O mixing ratio. The process of descent followed by isentropic mixing (process (2)) is illustrated schematically in Figure 3. During winter large scale subsidence takes place inside the vortex, which is relatively well isolated from extra-vortex air (e.g. Abrams et al, 1996). As the vortex weakens and finally breaks up during spring, air masses from outside the vortex irreversibly mix with vortex air along surfaces of constant potential temperature (e.g. Waugh et al., 1997). The effect of process (2) on the NO_y / N_2O correlation is illustrated by the dashed arrow in Figure 1. Mixing of two air masses at the same potential temperature in varying degrees (one air mass from inside the vortex, the other from outside) would lead to a linear relationship between NO_y and N_2O. If the reference tracer / tracer relation is non-linear, the mixing between these air masses can produce a new tracer / tracer relation quite

different than the reference relation (Waugh et al., 1997; Herman et al., 1998; Kondo et al., 1998; Michelsen et al., 1998). The combination of denitrification and mixing (process (3)) is illustrated by the dotted arrow in Figure 1. In this scenario, denitrification first reduces the NO_y mixing ratio at constant N_2O (illustrated by the part of the dotted arrow that is parallel to the NO_y axis). Subsequent mixing with extra-vortex air (illustrated by the rest of the dotted arrow) then would produce the observed air mass properties.

3.2. CH_4 / N_2O relationship

Michelsen et al. (1998) showed that mixing of subsided inner-vortex air with extra-vortex air is tends to reduce the curvature of the CH_4 / N_2O relation. We use straight mixing lines in the CH_4 / N_2O relation at specific potential temperature levels to quantify the amount of descent that has occurred inside the vortex and the degree of mixing between vortex and extra-vortex air for the regions sampled by the ER-2. MkIV measurements of the CH_4 / N_2O correlation (red circles in Figure 4) obtained near 65° N on May 8, 1997 for extra-vortex air are used as the extra-vortex reference correlation. The MkIV CH_4 / N_2O correlation agrees well with that measured by ATMOS in November 1994 between 40 and 50° N (Chang et al., 1996). A pronounced curvature is visible in the extra-vortex CH_4 / N_2O correlation for mixing ratios of N_2O below 250 ppbv. In contrast, observations obtained on April 26, 1997 near 20 km by the ER-2 ALIAS instrument reveal a nearly linear correlation between CH_4 and N_2O (green crosses in Figure 4) that deviates significantly from the extra-vortex correlation. The low mixing ratios of N_2O between 500 and 510 K potential temperature indicate that subsided polar vortex air masses were sampled during this ER-2 flight.

Since the correlation between the mixing ratios of these long-lived tracers cannot be changed by reversible transport or chemistry, the most obvious explanation for the ER-2 observations is mixing of extra-vortex air with polar vortex air that has subsided from higher altitudes (e.g. Waugh et al., 1997). The two air masses that must have mixed to produce the observed CH_4 / N_2O relations along the linear mixing line are referred to as the "inner-vortex end-member" and the "extra-vortex end-member". It is reasonable to assume that the bulk of the mixing took place in spring, following strongest descent within the vortex (this assumption is discussed below). Therefore the composition of the extra-vortex end-member (the trapezoid marked in Figure 4) is defined by the ambient mixing ratios of CH_4 and N_2O observed outside of the vortex by the ER-2 and the MkIV instrument at the same potential temperature level of the ER-2 flight. The composition of the inner-vortex end-member is defined by the intersection of the extrapolated ER-2 mixing line and the MkIV reference correlation (oval region in Figure 4). The CH_4 / N_2O relation is nearly linear between 15 and 40 ppbv N_2O. Therefore inhomogenous descent inside the polar vortex followed by mixing within the vortex of the air masses from different origins would not change the properties of the inner-vortex end-member considerably. The fractional contribution of the inner-vortex and the extra-vortex end-members to specific ER-2 observations along the CH_4 / N_2O mixing line is determined from the relative distance of the observed N_2O mixing ratio to that of both end-members.

3.3. Calculation of NO_y**

The mixing ratio of NO_y that would have been present in the absence of denitrification ac-

counting for the effects of descent and isentropic mixing is referred to here as NO_y**. This quantity differs from NO_y* which is based only on the refernce correlation and does not account for descent and mixing. The value of NO_y** is calculated on a point-by-point basis along the flight track of the ER-2 by considering mixing between the inner-vortex and extra-vortex end-members derived from our analysis of simultaneous measurements of CH_4 and N_2O. The mixing ratio of N_2O associated with the inner-vortex end-member (here defined as $[N_2O]_i$) was calculated based on the intersection of the straight line passing through a point defined by the measured mixing ratios of CH_4 and N_2O and a point defined by the extra-vortex end-member. The composition of the extra-vortex end-member used for all ER-2 observations considered here, which were obtained for potential temperatures between 500 and 530K, is defined by the trapezoid in Figure 4. The NO_y mixing ratios of both end-members can be estimated from the respective mixing ratios of N_2O and the NO_y / N_2O correlation measured by the MkIV instrument on May 8, 1997. Values of NO_y** have been calculated from the NO_y mixing ratios of both end-members and their fractional contribution to the mixed air-mass:

$$NO_y^{**} = \frac{[N_2O] - [N_2O]_i}{[N_2O]_e - [N_2O]_i} \cdot [NO_y]_e + \left(1 - \frac{[N_2O] - [N_2O]_i}{[N_2O]_e - [N_2O]_i}\right) \cdot [NO_y]_i \qquad (1)$$

where $[N_2O]$ denotes the mixing ratio of N_2O of the respective air mass, and the variables with indices *e* and *i* denote the properties of the extra-vortex and inner-vortex mixing end-member, respectively. The uncertainties of the calculated parameters including NO_y** have been estimated based on the uncertainty of the composition of the extra-vortex end-member (indicated by the size of the trapezoid in Figure 4) and the precisions of the measurements.

3.4. Underlying assumptions

Two critical assumptions for our analysis are: (a) the ability to directly combine remote (MkIV) and in-situ (ER-2 and OMS) observations of NO_y, CH_4, and N_2O aquired by vastly different techniques without corrections for possible systematic differences, and (b) the validity of the NO_y / N_2O and CH_4 / N_2O reference relations for conditions inside the Arctic vortex prior to significant isentropic mixing and denitrification. Assumption (a) is supported by the remarkably good agreement between the MkIV reference correlation for NO_y / N_2O and the ER-2 observations obtained in the Arctic vortex during January and February 1989 (Figure 2). Comparisons of MkIV and ER-2 observations of NO_y and N_2O obtained at mid-latitudes (Figure 2 of Sen et al., 1998) and of ATMOS and ER-2 observations of NO_y, CH_4 and N_2O (Figure 3 of Chang et al., 1996a; ATMOS acquires observations using solar occultation in a manner similar to the MkIV instrument) lend further confidence in the agreement of the different sources of data. Toon et al. (1998) conclude that the bias between the MkIV and ALIAS measurements of N_2O is only 2%. Finally, the excellent agreement between the MkIV CH_4 / N_2O reference relation and ALIAS II observations obtained at high latitude during POLARIS for extra-vortex air Herman et al. (1998) (discussed in section 3.3) provides additional support for the validity of assumption (a). Assumption (b) cannot be fully tested for the winter of 1996/97 since tracer measurements inside the Arctic vortex are not available during the formation phase in fall. However, assuming the validity of assumption (a), the in-situ observations of NO_y and N_2O obtained during January and February 1989 suggest that the MkIV NO_y / N_2O reference correlation is valid even during the initial phase of denitrification (Figure 2). We note that the re-

markably good agreement between the MkIV and in-situ observations of NO_y and N_2O supports the validity of both assumptions (a) and (b) because it would be highly unlikely that deviations from the assumptions would cancel in such a way to preserve the good agreement. Furthermore, the NO_y / N_2O and CH_4 / N_2O relations measured at northern mid-latitudes during November 1994 by ATMOS (Chang et al., 1996) agree well with the MkIV reference relations used here (the agreement between MkIV and ATMOS measurements of CH_4 and N_2O is discussed further in section 3.3). The validity of the additional assumption that most of the isentropic mixing occurs after the descent is supported by the observation that the potential temperature (based on the MkIV CH_4 / N_2O reference relation) associated with the extra-vortex end-members for the various ALIAS and ALIAS II mixing lines (Figure 4 and Section 3.3) is nearly identical to the potential temperature at which the in-situ measurements were obtained.

3.5. ER-2 flight on April 26, 1997

3.5.1. Descent and Mixing. Figure 5b shows the mixing ratio of N_2O calculated for the inner-vortex end-members along the ER-2 flight track on April 26, 1997. The mixing ratios of the inner-vortex end-member were found to be between 25 and 40 ppbv. The associated approximate altitudes from which the inner-vortex end-members subsided through the winter are approximately 32-34 km (Figure 5c). The altitudes have been estimated using the mixing ratios of N_2O and the MKIV extra-vortex profile of N_2O. An overall subsidence of approximately 13 km for air masses ending near 500 K (~20 km) is suggested by our analysis. This value agrees well with the overall descent of 13.8 km for air ending at 20 km that was derived by Abrams et al. (1996) for the Arctic winter 1992/93 from ATMOS / ATLAS-2 data. Abrams et al. (1996) showed that this descent is consistent with the theoretical results of Manney et al. (1994) and Rosenfield et al. (1994). The ratio between inner-vortex air and extra-vortex air in the sampled air masses has been calculated as described above and is shown in Figure 5d. For the observations discussed here, this ratio varies between 0.3 and 0.6 with higher fractions of inner-vortex air present at higher latitudes. As expected, high fractions of inner-vortex air correlate with high values of potential vorticity (Figure 5a).

3.5.2. Denitrification. Figure 5e compares observations of NO_y to NO_y* (NO_y based on the reference correlation) and NO_y** (NO_y calculated from the reference correlation, allowing for descent and isentropic mixing). Large differences between observed NO_y and NO_y* are apparent. In contrast, observations of NO_y agree well with NO_y** during most parts of the flight. This result shows that most of the NO_y deficit found along the ER-2 flight track was caused by descent followed by isentropic mixing. However, during the northermost part of the ER-2 flight the mixing ratios of NO_y were smaller than NO_y**, indicating that some denitrification had taken place. This is further investigated in Figure 6, where the observed NO_y / N_2O correlation, the NO_y** / N_2O correlation, and the extra-vortex reference correlation are shown.

Measured NO_y agrees well with NO_y** for N_2O mixing ratios larger than 125 ppbv. For N_2O levels below 100 ppbv, a deficit of measured NO_y compared to NO_y** is visible. This 1-2 ppbv deficit in NO_y is interpreted as the result of weak irreversible denitrification that occured earlier in the winter. Since the denitrification probably occured before the bulk of the mixing, it is reasonable to suggest that the deficit of NO_y originally caused by the denitrification was diluted by the subsequent mixing. Backprojection of the NO_y deficit to the pre-mixing conditions (dashed

lines in Figure 6) shows that the original average degree of denitrification must have been approximately 2-3 ppbv (solid arrow in Figure 6) to cause the NO_y deficit observed in late April. Most likely the denitrification inside the polar vortex was characterized by patchy regimes of higher denitrified areas and areas without denitrification (as was observed on February 7, 1989; see Figure 2). In the weeks following the denitrification events, comparatively fast mixing inside the vortex probably led to an averaging of the degree of denitrification throughout the vortex yielding the 2-3 ppbv level of denitrification reported above.

The weak denitrification reported here is consistent with the temperature structure of the 1996/1997 winter. PSC particles must grow to large sizes (on the order of 1 to 2 μm) to sediment with appreciable velocities (e.g. Salawitch et al., 1989). Particle formation and growth models show that PSC particles reach sizes large enough to cause rapid denitrification once temperature falls below the frostpoint, due to efficient uptake of water (e.g. Drdla and Turco, 1991). Differential growth may also lead to large particles for temperatures that are above the frostpoint but below the NAT (nitric acid trihydrate) equilibrium temperature (T_{NAT}) (Salawitch et al., 1989). However, Santee et al. (1998) show that the phase change required to initiate differential growth most likely requires suppression of temperature below T_{NAT} continuously for a period of at least several days. In the Arctic the cold temperature region is normally displaced from the center of the vortex. As air masses circulate in the vortex they alternately pass through cold ($T < T_{NAT}$) and warm regions every few days, so that severe denitrification in the Arctic may require the minimum temperature to drop below the frostpoint. Temperature analysis from the European Centre for Medium Range Weather Forecast shows that the synoptic temperatures dropped below the frostpoint (assuming 4.6 ppmv H_2O) only in limited areas (largest area less than $2x10^6$ km^2) and only for two short periods, both only a couple of days long during mid and late February. The potential for PSC II formation during 1996/97 was much smaller than in the winters of 1988/89 and 1995/96. The winter of 1995/96 is the coldest Arctic stratospheric winter on record (Naujokat and Pawson, 1997); the area covered by synoptic temperatures below the frostpoint was up to $4x10^6$ km^2 and very persistent (a first period persisted longer than three weeks in January 1996 and a second period about ten days during mid-February 1996). Furthermore, in 1996/97 the areas cold enough for synoptic PSC II formation were mainly at the 450 K level, which is below the air masses sampled by the ER-2 during its vortex flight. Considering some diabatic cooling during the late winter period, the air masses analysed by the ER-2 in late April at 500K would have been even somewhat above 500K during the cold periods in February. From vortex averaged radiative cooling rates calculated from the UGAMP model, it was estimated that the subsidence between the coldest period and the April ER-2 flight was between 5-10 K potential temperature.

Our analyses have been based on ER-2 measurements of N_2O obtained by the ALIAS instrument. In-situ measurements of the mixing ratio of N_2O are also obtained by the ATLAS (Airborne Tunable Laser Absorption Spectrometer) instrument for each ER-2 flight. There are slight differences between the ATLAS and ALIAS measurements of N_2O during limited segments of the two ER-2 flights considered here. However, we have repeated our entire analyses using the ATLAS measurements of N_2O and we note that our overall conclusions are independent of which measurement of N_2O is used.

3.6. ER-2 flight on June 30, 1997

During the ER-2 flight on June 30, 1997 remnants of the polar vortex were found at 510-530 K potential temperature, i.e. at slightly higher isentropic levels than during the flight of April 26. Figure 7 shows the CH_4 / N_2O relation measured during this flight. The inner-vortex end-members that contributed to the air mass probed by the ER-2 had fairly constant N_2O mixing ratios of about 15-20 ppbv (Figure 8a). The associated initial altitude is approximately 37 km (Figure 8b), so that the overall descent for air masses ending at around 520 K in June is estimated to be approximately 16 km. Figure 8c shows that the fraction of inner-vortex air in the probed air masses varied between 20 and 70 % for the air masses discussed here. The NO_y observations agree very well with NO_y** throughout the flight (Figure 9). This analysis reveals that the large deficits of NO_y compared with the extra-vortex reference can be explained entirely by descent and mixing. No indication for denitrification was found.

The vortex air masses sampled during the June 30, 1997 ER-2 flight were at higher potential temperature levels than those encountered during the April 26, 1997 flight. These air masses were well above the cold temperature region in February and synoptic temperatures never dropped below the frostpoint in these air masses. Our finding that they have not been significantly denitrified is consistent with the temperature structure of the 1996/97 winter.

3.7. OMS flight on June 30, 1997

On the same day as the latter ER-2 flight, the OMS balloon borne platform measured a profile of several trace species and encountered polar vortex remnants in two altitude regions around 500-520 K and 615-637 K potential temperature (Herman et al., 1998). The measured CH_4 / N_2O mixing ratios obtained during the balloon descent are plotted in Figure 10 together with the extra-vortex reference measured by the MkIV instrument. The ALIAS II observations are grouped into potential temperature ranges that are plotted in different colors.

The vortex air masses found around 495-520 K (blue in Figure 10) lie along a mixing line very similar to that formed by the ER-2 observations obtained on the same day. The measurements in air masses that have not been influenced by the polar vortex (black in Figure 10) agree remarkably well with the measurements of the MkIV instrument on May 8, 1997 (see also Herman et al., 1998). These observations strongly support the assumption that the measurements from the different platforms may be compared directly.

We now focus on the air masses probed between 615 and 637 K potential temperature (green in Figure 10). The CH_4 / N_2O relation of these air masses form a mixing line with a steeper slope than those indicated by the ER-2 and OMS measurements at lower altitudes. The mixing line meets the CH_4 / N_2O reference correlation at mixing ratios that correspond to the MkIV measurement obtained at 615 K potential temperature. This level coincides well with the potential temperature range probed by the OMS platform for the mixing line. The slope of the mixing line indicates that the inner-vortex end-member originated from well above the altitude region sampled by the MkIV instrument (dashed arrow in Figure 10). We used data from ATMOS/ATLAS-3 obtained during November of 1994 to identify the intersection of the extended mixing line with the reference correlation of CH_4 / N_2O (Figure 11). The intersection of the dashed line in Figure 11 with the extra-vortex reference indicates that the inner-vortex mixing member orig-

inated at an extremely low mixing ratio of N_2O and at a CH_4 mixing ratio of about 200 ppbv. Figure 12 shows that such low CH_4 levels are normally found above 50 km altitude. This result indicates that the air masses probed by the OMS platform between 615 and 637 K are the result of mixing of extra-vortex air with mesospheric air, which descended inside the polar vortex. The altitude region where we found indications for mesospheric air is only slightly below the altitude region of 630-670K, where Rinsland et al. (1998) reported a pocket of elevated mixing ratios of CO in April 1993, which also have been interpreted as the presence of subsided mesospheric air in the polar vortex in the middle stratosphere (Rinsland et al., 1998).

The NO_y / CH_4 correlation measured by ATMOS/ATLAS-3 between 40 and 50° N (Figure 13, 50° N is the highest latitude reached by the ATMOS instrument during the ATLAS-3 mission) has been used to calculate NO_y** from the estimated CH_4 mixing ratios of the inner-vortex end-member for the air masses probed by the OMS platform between 615 and 637 K potential temperatures (Figure 14). This figure shows that above 600 K quite low NO_y / N_2O ratios can be produced purely by mixing processes between subsided mesospheric air masses with extra-vortex air. This result supports the hypothesis of Kondo et al. (1998) that, for altitudes above 20 km low values of NO_y can easily be mistaken for severe denitrification if dynamical processes are neglected.

4. Conclusions

Mixing processes between subsided air masses from the polar vortex and mid-latitude air can considerably alter otherwise well established tracer correlations if their relationship is non-linear. The combined measurements of NO_y, N_2O and CH_4 obtained by the NOAA NO_y and the ALIAS instrument aboard the ER-2, the MkIV balloon-borne FTIR-spectrometer and the ALIAS II balloon borne tunable diode laser instrument during the POLARIS campaign provide detailed in-situ tracer data in the mixed air masses as well as concurrently measured reference correlations for extra-vortex air.

We developed a new technique for estimating the degree of denitrification in vortex air masses that have been mixed with extra vortex air. The technique is based on near linear mixing lines in the otherwise non-linear correlation between CH_4 and N_2O to quantify the subsidence and mixing that led to the properties of the mixed air masses. The mixing lines at increasing potential temperature levels show an increasing slope and intersect with the reference correlation at their respective potential temperature, supporting the key assumptions required for our analysis. The information extracted from the CH_4 / N_2O correlation has been used to predict the abundance of NO_y** (the expected mixing ratio of NO_y accounting for descent and isentropic mixing) for the mixed air masses. The degree of denitrification has been derived by comparing observed NO_y with NO_y**. Our analysis reveals evidence for only a small degree of denitrification in a limited region of the Arctic vortex sampled by the ER-2 flight on April 26, 1997 and no indication for denitrification for vortex air sampled during a flight on June 30, 1997. The considerable deficit of NO_y compared with NO_y* (the mixing ratio of NO_y derived from the abundance of N_2O without considering mixing) during both flights, which would have been incorrectly interpreted as the result of denitrification in the "traditional" approach, is actually mainly the result of descent and end-member mixing.

During an OMS balloon flight on June 30, 1997 remnants of the polar vortex have been found at two levels. The CH_4 / N_2O mixing line found around 620 K potential temperature reveals that the air mass at this level was formed by mixing between descended mesospheric air and extra-vortex air. The mixing ratio of NO_y** estimated from subsidence and mixing for these air masses is as low as 7 ppbv at N_2O levels between 50 and 75 ppbv, compared to NO_y*, which is ~16 ppbv at these levels of N_2O. This result suggests that had a measurement of NO_y been available on the OMS platform it could have been mistaken for denitrification if it had only been compared to NO_y*.

Our analysis demonstrates the importance of using measurements of additional conserved species to be able to accurately interpret changes in the NO_y / N_2O relation with respect to denitrification. The main uncertainty in this work lies in the definition of the unmixed inner-vortex reference correlations that had been present during the build up phase of the vortex in fall. We present data obtained inside the vortex near 20 km during a previous winter to support the validity of the reference relations used in this analyses. However, high reaching balloon measurements of tracer profiles inside the early vortex would largely reduce the uncertainty of these type of analyses.

Acknowledements. We thank P. Newman and L. Lait for providing the potential vorticity data used in Figure 5. Part of the research described in this paper was carried out by the Jet Propulsion Laboratory, California Institute of Technology, under a contract with the National Aeronautics and Space Administration.

References

Abrams, M.C., G. L. Manney, M. R. Gunson, M. M. Abbas, A. Y. Chang, A. Goldman, F. W. Irion, H. A. Michelsen, M. J. Newchurch, C. P. Rinsland, R. J. Salawitch, G. P. Stiller, and R. Zander, Trace gas transport in the Arctic vortex inferred from ATMOS ATLAS 2 observations during April 1993, Geophys. Res. Let., 23, 2341-2344, 1996.

Arnold, F., K. Gollinger, and S. Spreng, *title*, in Polar Stratospheric Ozone (eds Pyle, J. A. et al.) 175-178 (Rep. 56, Commissions of the European Communities, DG-XII, Brussels, 1996).

Brune, W. H., D. W. Toohey, J. G. Anderson, K. R. Chan, In situ observations of ClO in the Arctic stratosphere: ER-2 aircraft results from 59°N to 80°N latitude, Geophys. Res. Let., 17, 505-508, 1990.

Brune, W. H., J. G. Anderson, D. W. Toohey, D. W. Fahey, S. R. Kawa, R. L. Jones, D. S. McKenna, and L. R. Poole, The potential for ozone depletion in the Arctic polar stratosphere, Science, 252, 1260-1266, 1991.

Chang, A.Y., R.J. Salawitch, H.A. Michelsen, M.R. Gunson, M.C. Abrahms, R. Zander, C.P. Rinsland, M. Loewenstein, J.R. Podolske, M.H. Proffitt, J.J. Margitan, D.W. Fahey, R.-S. Gao, K.K. Kelly, J.W. Elkins, C.R. Webster, R.D. May, K.R. Chan, M.M. Abbas, A. Goldman, F.W. Irion, G.L. Manney, M.J. Newchurch, and G.P. Stiller, A comparison of measurements from ATMOS and instruments aboard the ER-2 aircraft: Tracers of atmospheric

transport, Geophys. Res. Lett., 23, 2389-2392, 1996a.

Chang, A.Y., R.J. Salawitch, H.A. Michelsen, M.R. Gunson, M.C. Abrahms, R. Zander, C.P. Rinsland, J.W. Elkins, G.S. Dutton, C.M. Volk, C.R. Webster, R.D. May, D.W. Fahey, R.-S. Gao, M. Loewenstein, J.R. Podolske, R.M. Stimpfle, D.W. Kohn, M.H. Proffitt, J.J. Margitan, K.R. Chan, M.M. Abbas, A. Goldman, F.W. Irion, G.L. Manney, M.J. Newchurch, and G.P. Stiller, A comparison of measurements from ATMOS and instruments aboard the ER-2 aircraft: Halogenated gases, Geophys. Res. Lett., 23, 2393-2396, 1996b.

Dessler, A. E., D. B. Considine, E. L. Flemming, C. H. Jackman, M. R. Schoeberl, A generalized view of the interrelationship between the abundances of long-lived trace species in the stratosphere, submitted.

Drdla, K, and R. P. Turco, Denitrification through PSC formation - a 1-D model incorporating temperature oscillations, J. Atmos. Chem., 12, 319-366, 1991.

Fahey, D. W., *et al.*, In situ measurements of total reactive nitrogen, total water, and aerosol in a polar stratospheric cloud in the Antarctic, J. Geophys. Res., 94, 11299-11315, 1989.

Fahey, D. W., K. K. Kelly, S. R. Kawa, A. F. Tuck, M. Loewenstein, K. R. Chan, and L. E. Heidt, Observations of denitrification and dehydration in the winter polar stratospheres, Nature, 344, 321-324, 1990

Kawa S. R., D. W. Fahey, L. E. Heidt, W. H. Pollock, S. Solomon, D. E. Anderson, M. Loewenstein, M. H. Poffitt, J. J. Margitan, and K. R. Chan, Photochemical partitioning of the reactive nitrogen and chlorine reservoirs in the high-latitude stratosphere, J. Geophys. Res., 97, 7905-7923, 1992

Herman, R. L., D. C. Scott, C. R. Webster, R. D. May, E. J. Moyer, R. J. Salawitch, Y. L. Yung, G. C. Toon, B. Sen, J. J. Margitan, K. H. Rosenlof, H. A. Michelson, and J. W. Elkins, Tropical entrainment time scales inferred from stratospheric N_2O and CH_4 observations, Geophys. Res. Let., 25, 2781-2784, 1998.

Hintsa, E. J., P. A. Newman, H. H. Jonsson, C. R. Webster, R. D. May *et al.*, Dehydration and denitrification in the Arctic polar vortex during the 1995-1996 winter, Geophys. Res. Let., 25, 501-504, 1998

Huebler, G., D. W. Fahey, K. K. Kelly, D. D. Montzka, M. A. Carroll, A. F. Tuck, L. E. Heidt, W. H. Pollock, G. L. Gregory, and J. F. Vedder, Redistribution of reactive odd nitrogen in the lower Arctic stratosphere, Geophys. Res. Let., 17, 453-456, 1990.

Keim, E. R., M. Loewenstein, J. R. Podolske, D. W. Fahey, R. S. Gao, E. L. Woodbridge, R. C. Wamsley, S. G. Donnelly, L. A. Del Negro, C. D. Nevison, S. Solomon, K. H. Rosenlof, C. J. Scott, M. K. W. Ko, D. Weisenstein, and K. R. Chan, Measurments of the NO_y-N_2O correlation in the lower stratosphere: Latitudinal and seasonal changes and model comparisons, J. Geophys. Res., 102, 13193-13212, 1997.

Kondo, Y., M. Koike, A. Engel, U. Schmidt, M. Müller, T. Sugita, H. Kanzawa, T. Deshler, T. Nakazawa, S. Aoki, H. Irie, N. Toriyama, T. Suzuki, and Y. Sasano, NO_y-N_2O correlation inside the Arctic vortex in February 1997: Dynamical and chemical effects, submitted to J. Geophys. Res.

Loewenstein, M., J. R. Podolske, D. W. Fahey, E. L. Woodbridge, P. Tin, *et al.*, New observations of the NO_y / N_2O correlation in the lower stratosphere, Geophys. Res. Let., 2531-2534, 1993.

Naujokat B. and S. Pawson, The cold stratospheric winters 1994/95 and 1995/96, Geophys. Res. Let., 23, 3703-3706, 1996.

Nevison, C. D. and E. A. Holland, A reaxamination of the impact of anthropogenically fixed nitrogen on atmospheric N2O and the stratospheric O3 layer, J. Geophys. Res., 102, 25519-25537, 1997.

Notholt, J., P. von der Gathen, S. Peil, Heterogeneous conversion of HCl and $ClONO_2$ during the Arctic winter 1992/1993 initiating ozone depletion, J. Geophys. Res., 100, 11269-11274, 1995.

Manney, G. L., R. W. Zurek, A. O'Neill, and R. Swinbank, On the motion of air through the stratospheric polar vortex, J. Atmos. Sci., 51, 2973-2994, 1994.

Michelsen, H. A., G. L. Manney, M. R. Gunson, R. Zander, Correlations of stratospheric abundances of NOy, O3, N2O, and CH4 derived from ATMOS measurements, J. Geophys. Res., in press.

Oelhaf, H., G. Wetzel, T. von Clarmann, M. Schmidt, J. B. Renard, M. Pirre, E. Lateltin, P. Aimedieu, C. Phillips, F. Goutail, J.-P. Pommerau, Y. Kondo, T. Sugita, H. Nakajima, M. Koike, W. J. Williams, F. J. Mucray, P. Sullivan, A. Engel, U. Schmidt, and A. M. Lee, Correlative balloon measurements of the vertical distribution of N_2O, NO, NO_2, NO_3, HNO_3, N_2O_5, $ClONO_2$, and total reactive NO_y inside the polar vortex during SESAME, in Polar Stratospheric Ozone (eds Pyle, J. A. et al.) 175-178 (Rep. 56, Commissions of the European Communities, DG-XII, Brussels, 1996).

Plumb, R. A. and M. W. K. Ko, Interrelationships between mixing ratios of long-lived stratospheric constituents, J. Geophys. Res., 97, 10145-10156, 1992.

Rex, M., N. R. P. Harris, P. von der Gathen, R. Lehmann, G. O. Braathen, E. Reimer, A. Beck, M. P. Chipperfield, R. Alfier, M. Allaart, F. O'Conner, H. Dier, V. Dorokhov, H. Fast, M. Gil, E. Kyrö, Z. Litynska, I. S. Mikkelsen, M. G. Molineux, H. Nakane, J. Notholt, M. Rummukainen, P. Viatte, and J. Wenger, Prolonged stratospheric ozone loss in the 1995/96 Arctic winter, Nature, 389, 835-838, 1997.

Rinsland, C. P., R. J. Salawitch, M. R. Gunson, S. Solomon, R. Zander, E. Mahieu, A. Goldman, M. J. Newchurch, F. W. Irion, and A. Y. Chang, Polar stratospheric descent of NO_y and CO and Arctic denitrification during winter 1992-93, submitted to J. Geophys. Res.

Roche, A. E., J. B. Kummer, J. L. Mergenthaler, R. W. Nightingale, W. G. Uplinger, G. A. Ely, J. F. Potter, D. J. Wuebbels, P. S. Connel, *et al.*, J. Atmos. Sci., 51, 2877-2902, 1994.

Rosenfield, J. E., P. A. Newman, and M. R. Schoeberl, Computations of diabatic descent in the stratospheric polar vortex, J. Geophys. Res., 99, 16677-16689, 1994.

Russell III, J. M., C. B. Farmer, C. P. Rinsland, R. Zander, L. Froidvaux, G. C. Toon, B. Gao, J. Shaw, and M. Gunson, J. Geophys. Res., 93, 1718-1736, 1988.

Salawitch, R. J., G. P. Gobbi, S. C. Wofsy, and M. B. McElroy, Denitrification in the Antarctic stratosphere, Nature, 339, 525-527, 1989.

Salawitch, R. J., M. B. McElroy, J. H. Yatteau, S. C. Wofsy, M. R. Schoeberl, L. R. Lait, P. A. Newman, K. R. Chan, M. Loewenstein, J. R. Podolske, S. E. Strahan, and M. H. Proffitt, Geophys. Res. Let., 17, 561-564, 1990.

Salawitch, R. J., S. C. Wofsy, E. W. Gottlieb, L. R. Lait, P. A. Newman, M. R. Schoeberl, M. Loewenstein, J. R. Podolske, S. E. Strahan, M. H. Proffitt, C. R. Webster, R. D. May, D. W. Fahey, D. Baumgartner, J. E. Dye, J. C. Wilson, K. K. Kelly, J. W. Elkins, K. R. Chan, J. G. Anderson, Chemical loss of ozone in the Arctic polar vortex in the winter of 1991-1992, Science, 261, 1146-1149, 1993.

Santee, M. L., W. G. Reed, J. W. Waters, L. Froidvaux, G. L. Manney, D. A. Flower, R. F. Jarnot, R. S. Harwood, and G. E. Peckham, Interhemispheric differences in polar stratospheric HNO_3, H_2O, ClO, and O_3, Science, 267, 849-852, 1995.

Santee, M. L., A. Tabazadeh, G. L. Manney, R. J. Salawitch, L. Froidvaux, W. G. Read, and J. W. Waters, UARS Microwave Limb Sounder HNO3 observations: Implications for Antarctic polar stratospheric clouds, J. Geophys. Res., 103, 13285-13313, 1998.

Sen B., G.C. Toon, J.-F. Blavier, E.L. Fleming and C.H. Jackman, Balloon-borne observations of midlatitude fluorine abundance, J. Geophys. Res.,101, 9045-9054, 1996.

Sen B., G.C. Toon, G.B. Osterman, J.-F. Blavier, J.J. Margitan and R.J. Salawitch, Measurements of reactive nitrogen in the stratosphere, J. Geophys. Res., 103, in press, 1998.

Toon G. C., et al., Infrared aircraft measurements of stratospheric composition over Antarctica during September 1987, J. Geophys. Res, 94, 16571-16596, 1989.

Toon G. C., The JPL MkIV interferometer, Optics and Photonics News, 2, 19-21, 1991.

Toon, G. C., C. B. Farmer, P. W. Schaper, L. L. Lowes, and R. H. Norton, Composition measurements of the 1989 Arctic winter stratosphere by airborne infrared solar absorption spectroscopy, J. Geophys. Res., 97, 7939-7961, 1992.

Toon et al., in preparation.

Toon, O. B., P. Hamill, R. P. Turco, and J. Pinto, Condensation of HNO3 and HCl in the winter polar stratospheres, Geophys. Res. Let., 13, 1284-1287, 1986.

Hermann, R.L. et al., Tropical entrainment time scales inferred from stratospheric N_2O and CH_4 observations, Geophys. Res. Lett., 25, 2781-2784, 1998.

Waters, J. W., L. Froidvaux, W. G. Read, G. L. Manney, L. S. Elson, D. A. Flower, R. F. Jarnot, and R. S. Harwood, Stratospheric ClO and ozone from the Microwave Limb Sounder on the Upper Atmosphere Research Satellite, Nature, 362, 597-602, 1993.

Waugh, D. W., R. A. Plumb, J. W. Elkins, D. W. Fahey, K. A. Boering, G. S. Dutton, C. M. Volk, E. Keim, R.-S. Gao, B. C. Daube, S. C. Wofsy, M. Loewenstein, J. R. Podolske, K. R. Chan, M. H. Proffitt, K. K. Kelly, P. A. Newman, and L. R. Lait, Mixing of vortex air into middle latitudes as revealed by tracer-tracer scatterplots, J. Geophys. Res., 102, 13119-13134, 1997.

Webster, C. R., R. D. May, D. W. Toohey, L. M. Avallone, J. G. Anderson, P. Newman, L. Lait, M. R. Schoeberl, J. W. Elkins, and K. R. Chan, Chlorine chemistry on polar stratospheric cloud particles in the Arctic winter, Science, 261, 1130-1133, 1993

Webster, C.R., R.D. May, C.A. Trimble, R.G. Chave and J. Kendall, Aircraft (ER-2) laser infrared absorption spectrometer (ALIAS) for in situ stratospheric measurements of HCl, N_2O, CH_4, NO2 and HNO3, Applied Optics 33, 454-472, 1994.

Figure 1: NO_y / N_2O correlations measured during the MkIV flight on May 8, 1997 and during the ER-2 flight on April 26, 1997. The MkIV data represent a vertical profile between 8 and 37 km altitude. The potential temperatures of some data points are indicated in the plot. The error bars denote the 1σ precision of the MkIV measurements. All ER-2 data points have been measured between potential temperatures of 500 and 510 K. The ER-2 NO_y measurements were obtained by the NOAA chemilumescence instrument with a 1 σ total uncertainty of better than 10 %; the ER-2 N_2O measurements were made by the ALIAS diode laser instrument with a 1σ total uncertainty of 5% (1% precision). The dashed, dotted and dash-dotted lines illustrate scenarios with different degrees of denitrification and descent that could explain the low mixing ratios of NO_y observed by the ER-2 at mixing ratios of N_2O below 100 ppbv.

Figure 2: As in Figure 1, but for ER-2 data measured during an early winter and a mid-winter flight during AASE in 1989. The ER-2 data has not been filtered by Θ. The ER-2 observations of N_2O were obtained by the ATLAS instrument with a 1 σ total uncertainty of 3%. They were obtained for temperatures above T_{NAT}. However, the average temperature near 20 km during January 1989 was lower than observed during the 26 years prior to 1989 and the minimum tem-

perature in the vortex was persistently below T_{NAT} and reached the frostpoint during late January 1989 (Nagatani et al., 1990). Fits to ER-2 observations in northern mid-latitudes in various years and seasons (Keim et al, 1997) are also shown (black lines). The ER-2 data was normalized to 1997, assuming an increasing trend in the N_2O and NO_y mixing ratios of 0.2% per year.

Figure 3: Illustration of the large scale descent in the polar vortex, which brings air masses from high altitudes to low potential temperature levels where they can mix with extra-vortex air mainly during the late vortex and vortex break up period. In the right hand panel the descended inner-vortex mixing member is marked by an "i" and the extra-vortex mixing member is marked by an"e". To predict the properties of the mixed air masses, the original level of the air mass "i" has to be estimated.

Figure 4: CH_4 / N_2O correlation measured by the MkIV on May 8, 1997 and the ER-2 ALIAS instrument on the same flight as in Figure 1. The 1 σ total uncertainty of both the ALIAS CH_4 and N_2O measurements is 5% (1% precision). The error bars for the MkIV measurement denote the 1σ precision. The mixing line for the ER-2 measurements is indicated by the dotted line. The regions where the mixing line intersects the extra-vortex reference correlation denote the air masses that have mixed to produce the properties observed by the ER-2 along the mixing line. The inner- and extra-vortex mixing end-members are indicated. The altitudes and potential temperatures of the MkIV measurements in these regions are shown.

Figure 5: Measured and calculated quantities along the northbound track of the ER-2 flight on April 26, 1997. The gray shaded areas give an estimate of the uncertainty based on the errors in the measurements and the uncertainty in defining the properties of the extra-vortex mixing end-member. (a) Potential vorticity (1 PVU = 10^{-6} K m^2 s^{-1} kg^{-1}), (b) Calculated mixing ratio of N_2O for the inner-vortex mixing end-member, (c) corresponding approximate early winter altitude of the inner-vortex air, (d) fraction of inner-vortex air vs. extra-vortex air in the mixed sample, (e) NO_y* which would have been predicted from the N_2O vmrs without considering mixing (blue), NO_y** predicted with consideration of mixing (red), and NO_y measured by the NOAA chemiluminescence instrument aboard the ER-2 (green).

Figure 6: MkIV and ER-2 measurements as in Figure 1. The NO_y** predicted for the air masses sampled by the ER-2 (red) and its uncertainty (gray, c.f. Figure 5) are compared with the measured NO_y (green). NO_y** was calculated from the degree of descent and mixing derived from the CH_4 / N_2O correlation. The NO_y vs. NO_y** deficit at low N_2O levels is interpreted as a signature of irreversible denitrification. The pre-mixing degree of denitrification in the air masses is estimated by a back-projection of the measured properties of the mixed sample to the properties of the inner-vortex mixing end-member (dashed lines). The estimated average

pre-mixing degree of denitrification in the sampled air masses is indicated by the arrow. Since the air masses inside the vortex are rapidly mixed and the denitrification typically occurs inhomogenously, this degree of denitrification is likely the result of mixing of more heavily denitrified air masses with less or non-denitrified inner-vortex air.

Figure 7: As Figure 4, but for the portion of the ER-2 flight at potential temperatures of 510-530 K near 65° N on June 30

Figure 8: As Figure 5, but for the portion of the ER-2 flight at potential temperatures of 510-530 K near 65° N on June 30.

Figure 9: As in Figure 6, but for the ER-2 flight on June 30, 1997. The vortex remnants were encountered while the ER-2 was between potential temperatures of 510 and 530 K; only ER-2 measurements between these levels have been plotted. No indication for denitrification is apparent.

Figure 10: CH_4 / N_2O correlation observed by the ALIAS II instrument during the OMS balloon flight on June 30, 1997, compared to the MkIV measurements on May 8, 1997. The ALIAS II OMS data has been grouped into extra-vortex samples (black) and measurements obtained during the penetration of two distinct layers of vortex air remnants (green: 615-637 K, blue: 495-520 K). The observations within the vortex remnants reveal distinct mixing lines (dashed) for both potential temperature regions. The MkIV measurements on May 8, 1997 are given in red. The potential temperatures of the MkIV data points at the intersections with the OMS mixing lines are indicated.

Figure 11: CH_4 / N_2O correlation for the OMS encounter of vortex remnants at 615 - 637 K potential temperature (green) compared with an extra-vortex reference correlation established by ATMOS/ATLAS-3 measurements obtained between 40 and 50° N in early November 1994 (blue dots, a fit to the data is plotted as blue line). The MkIV reference correlation from May 8, 1997 is shown in red.

Figure 12: CH_4 profile measured by ATMOS/ATLAS-3 between 40 and 50° N in early November 1994. The vertical line denotes the mixing ratio of CH_4 of the inner-vortex end-member for the OMS mixing line observed at 615-637 K potential temperature.

Figure 13: NO_y / CH_4 reference correlation measured by ATMOS/ATLAS-3 between 40 and 50° N in early November 1994. The fit to the data has been used to estimate the mixing ratio of NO_y of the inner-vortex mixing end-member based on the estimated mixing ratio of CH_4 of that air mass (c.f. Figure 10).

Figure 14: The NO_y** / N_2O correlation predicted for the air masses measured by OMS between 615 and 637 K on June 30 based on the degree of subsidence and mixing inferred from the CH_4 vs. N_2O correlation. No denitrification has been assumed. MkIV data as in Figure 1.

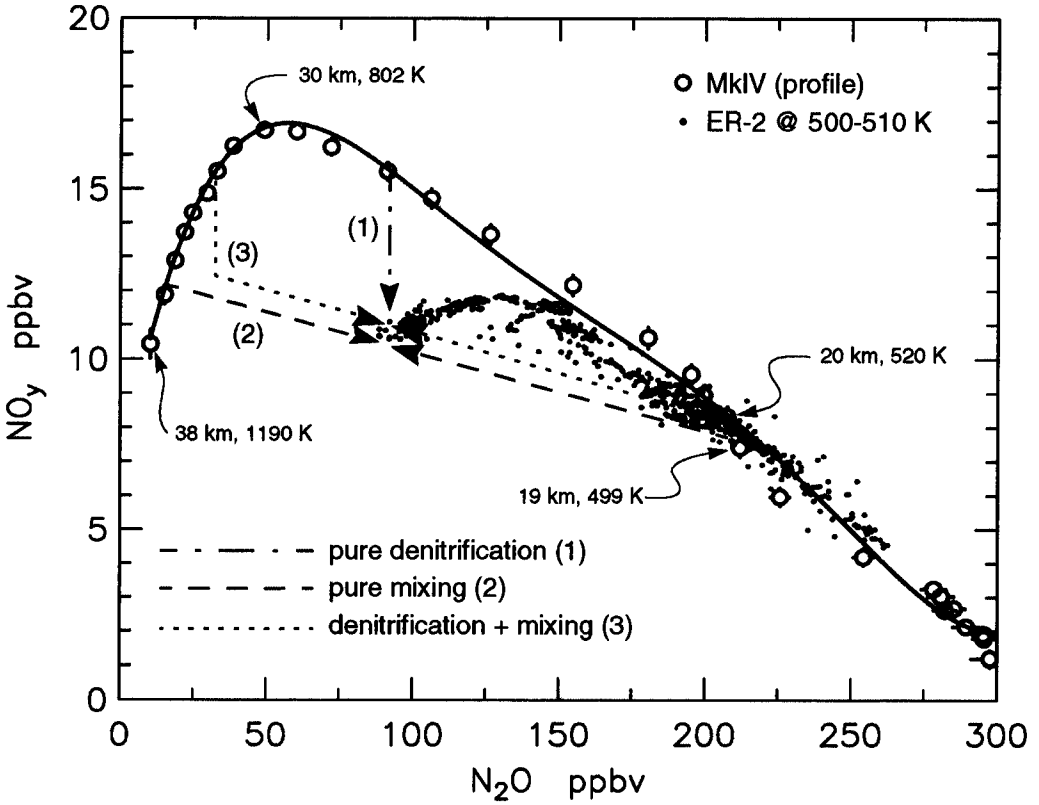
20
15
10
5
0
0
50
100
150
200
250
300
NO_y ppbv
N_2O ppbv
30 km, 802 K
MkIV (profile)
ER-2 @ 500-510 K
(1)
(2)
(3)
20 km, 520 K
38 km, 1190 K
19 km, 499 K
pure denitrification (1)
pure mixing (2)
denitrification + mixing (3)

Figure 1:

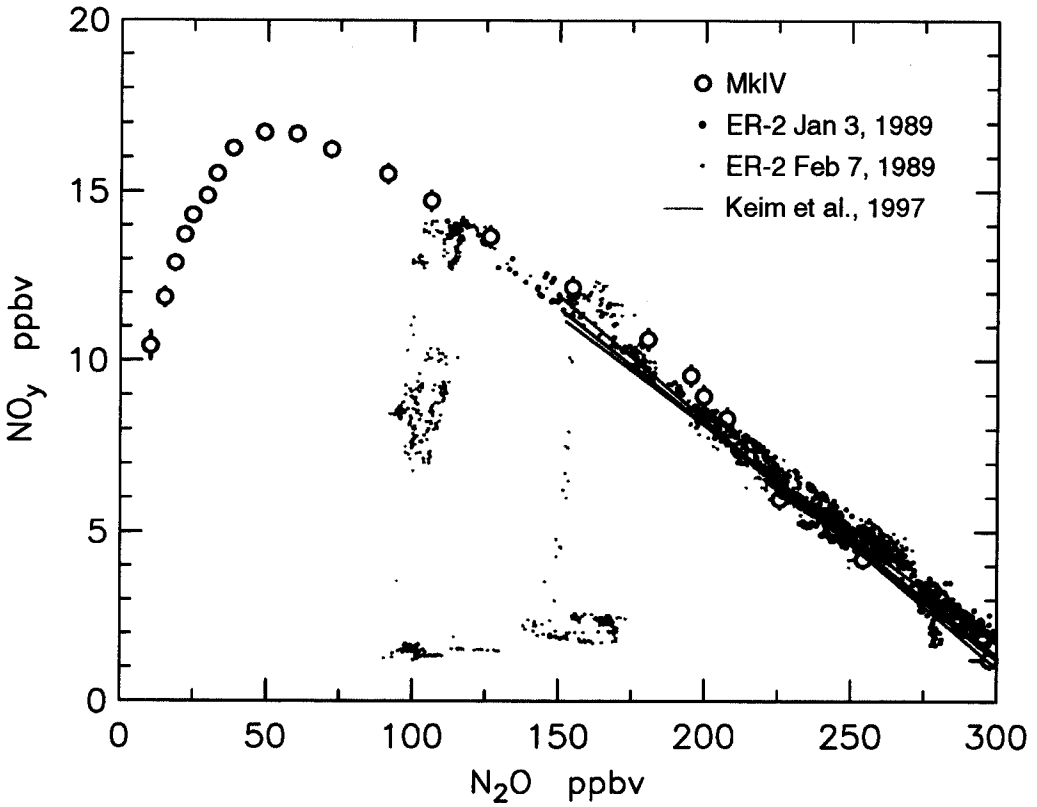
MkIV
ER-2 Jan 3, 1989
ER-2 Feb 7, 1989
Keim et al., 1997
NO_y ppbv
N_2O ppbv
0
5
10
15
20
0
50
100
150
200
250
300

Figure 2:

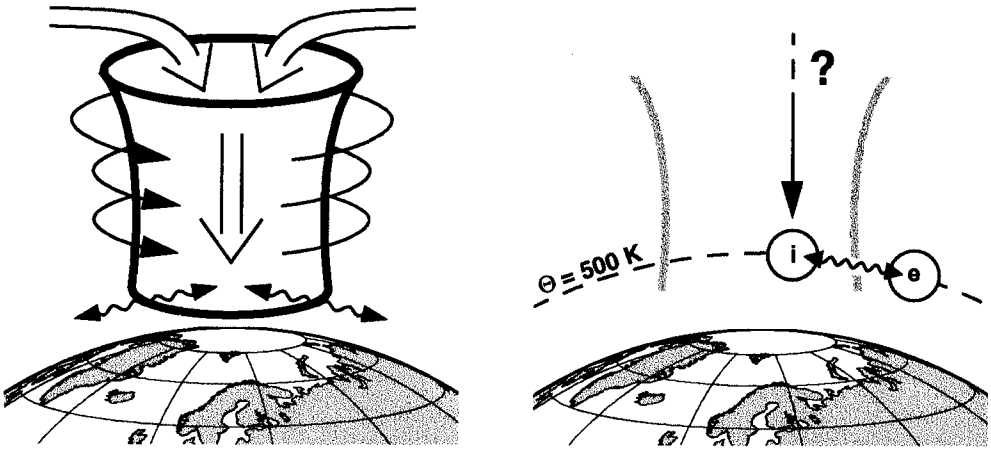

Figure 3:

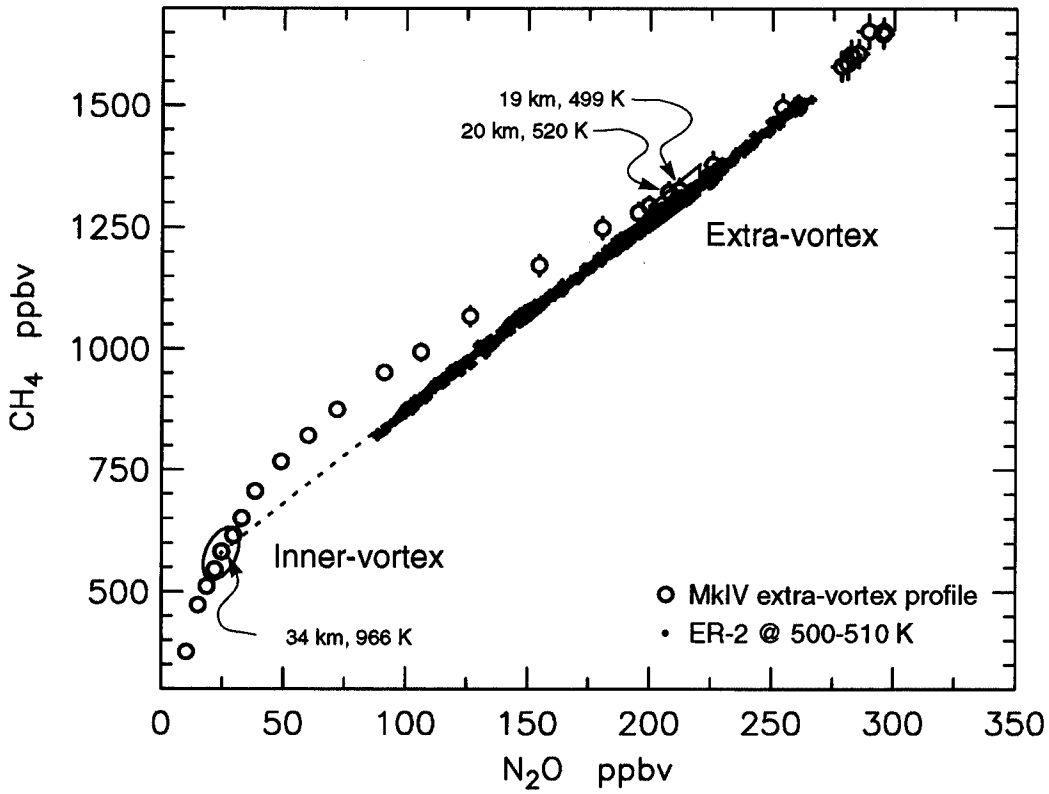
19 km, 499 K
20 km, 520 K
Extra-vortex
Inner-vortex
34 km, 966 K
MkIV extra-vortex profile
ER-2 @ 500-510 K
CH4 ppbv
N2O ppbv
1500
1250
1000
750
500
0
50
100
150
200
250
300
350

Figure 4:

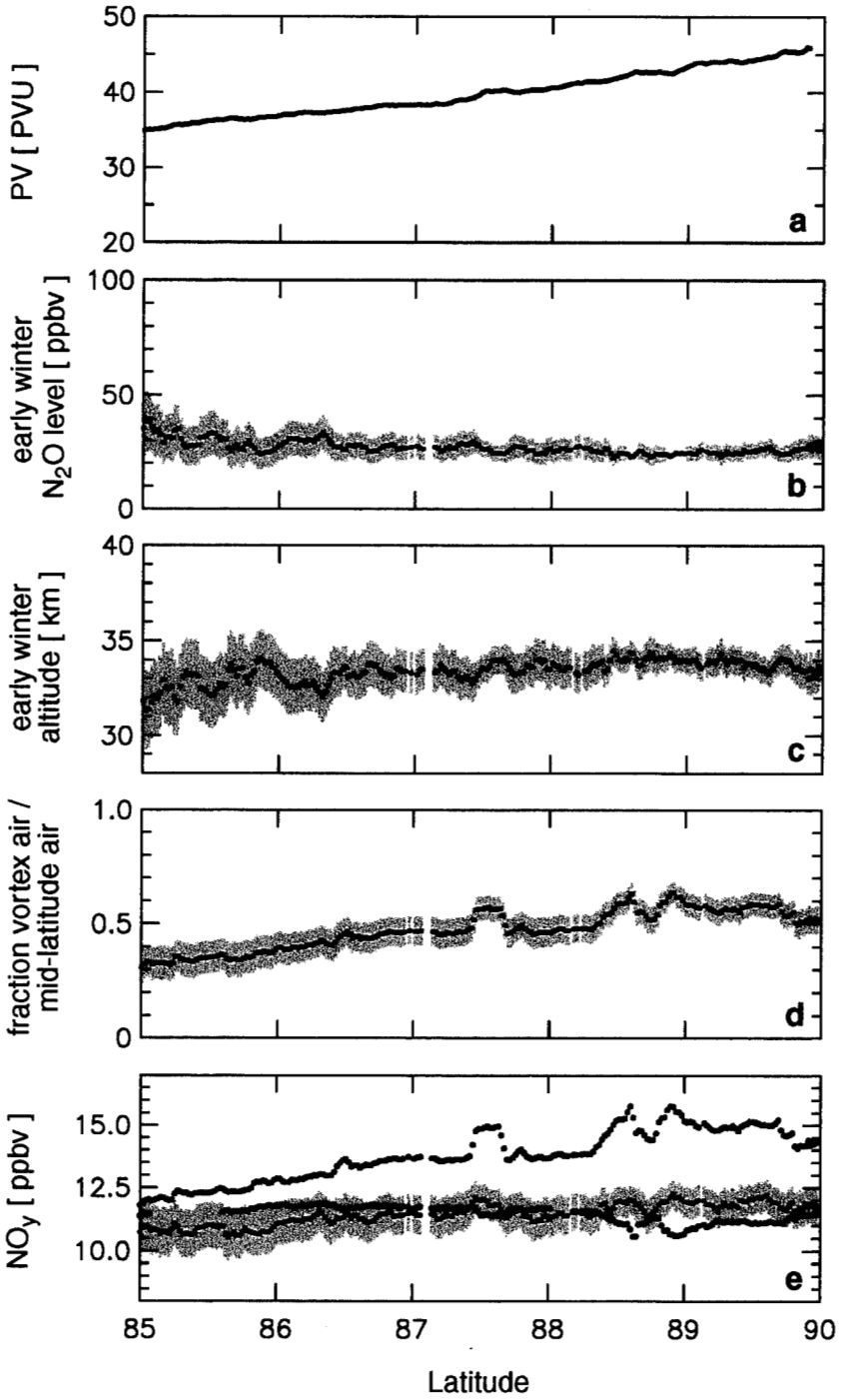
PV [PVU]
50
40
30
20
a
early winter
N_2O level [ppbv]
100
50
0
b
early winter
altitude [km]
40
35
30
c
fraction vortex air /
mid-latitude air
1.0
0.5
0
d
NO_y [ppbv]
15.0
12.5
10.0
e
85
86
87
88
89
90
Latitude

Figure 5:

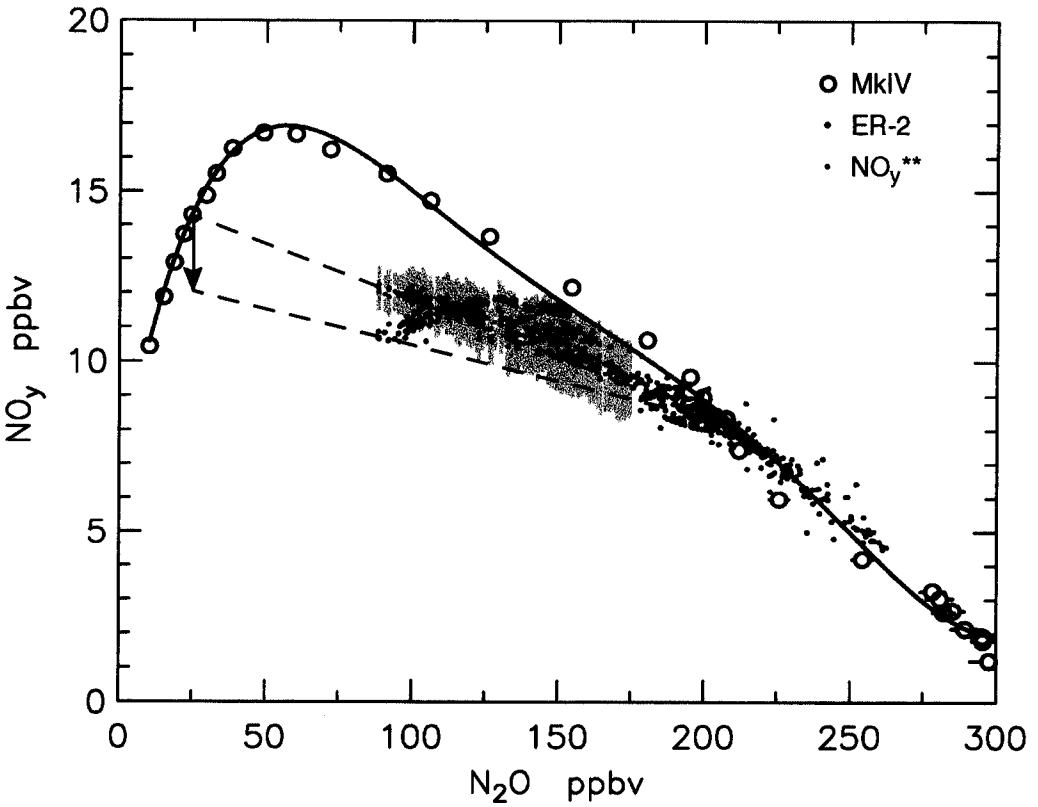
MkIV
ER-2
NOy**
NOy ppbv
N2O ppbv
0
5
10
15
20
0
50
100
150
200
250
300

Figure 6:

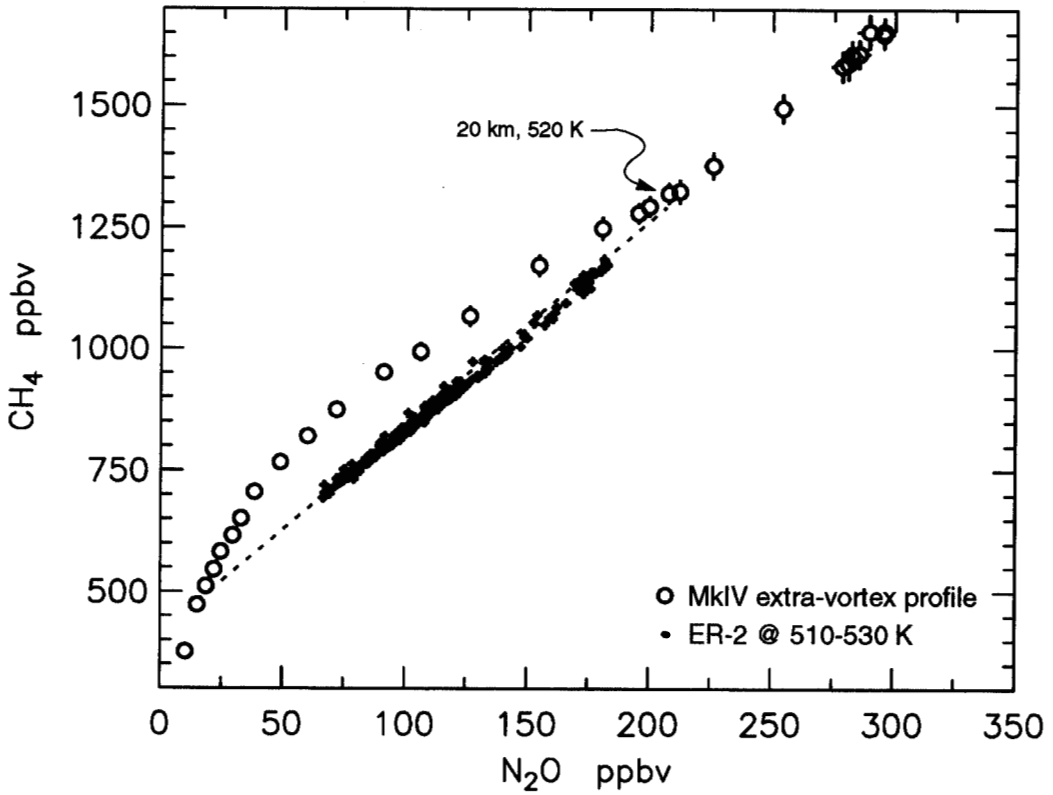
20 km, 520 K
MkIV extra-vortex profile
ER-2 @ 510-530 K
CH4 ppbv
N2O ppbv
1500
1250
1000
750
500
0
50
100
150
200
250
300
350

Figure 7:

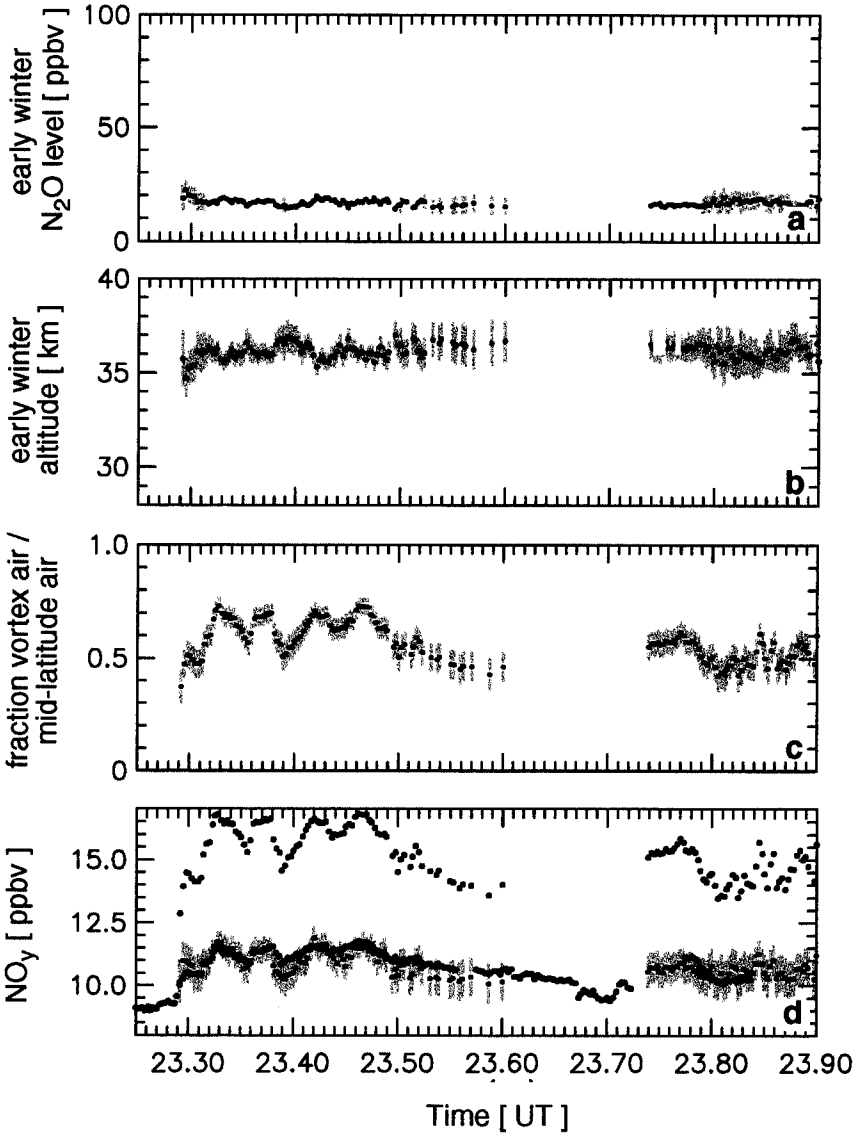
early winter
N_2O level [ppbv]
100
50
0
a
early winter
altitude [km]
40
35
30
b
fraction vortex air /
mid-latitude air
1.0
0.5
0
c
NO_y [ppbv]
15.0
12.5
10.0
d
23.30
23.40
23.50
23.60
23.70
23.80
23.90
Time [UT]

Figure 8:

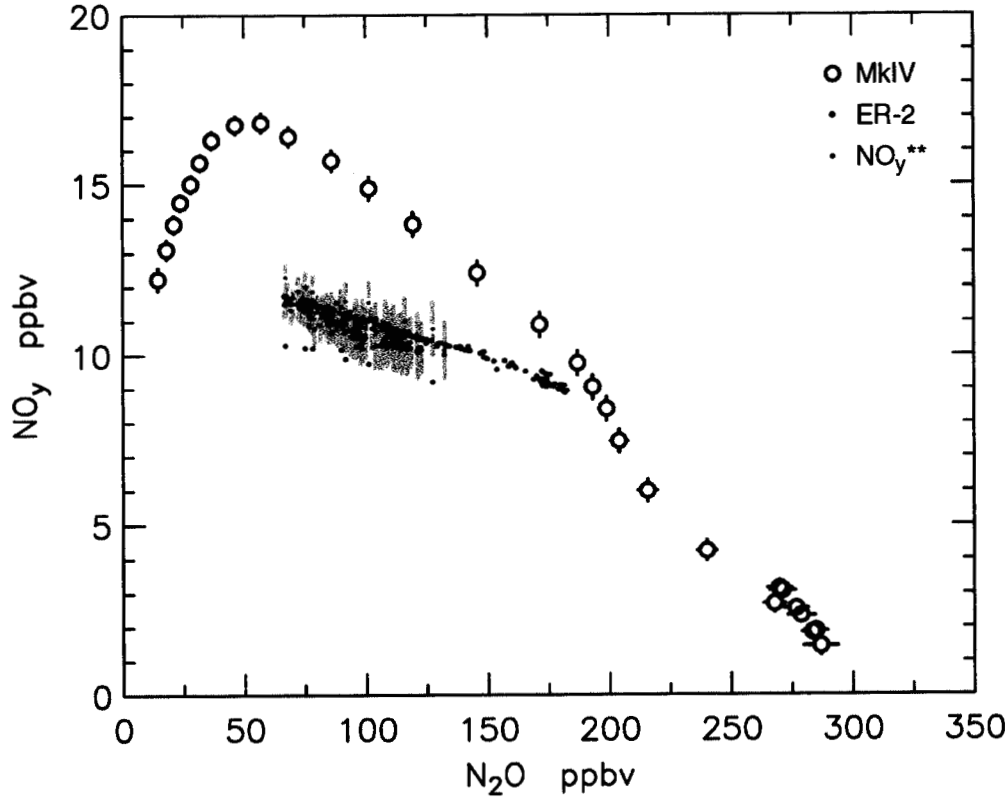
MkIV
ER-2
NO_y**
NO_y ppbv
N_2O ppbv
0
5
10
15
20
0
50
100
150
200
250
300
350

Figure 9:

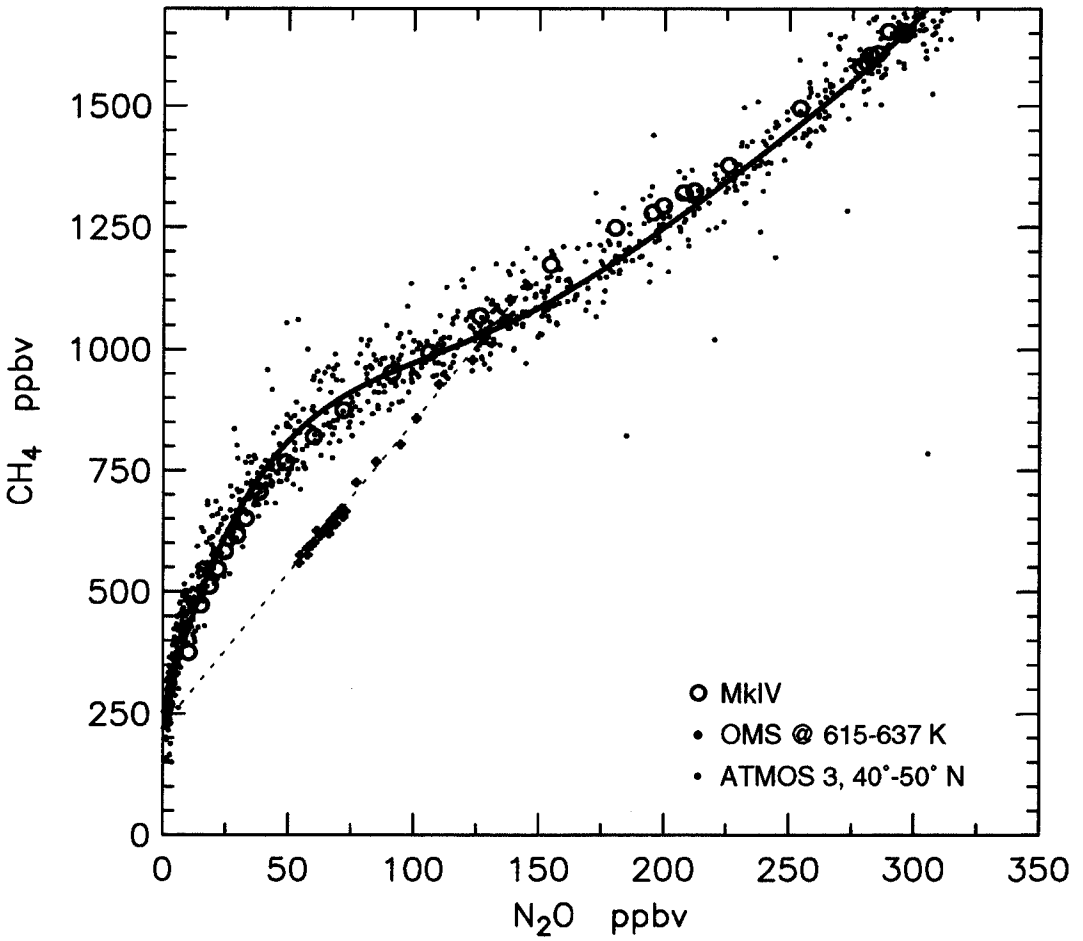
1500
1250
1000
750
500
250
0
CH_4 ppbv
0
50
100
150
200
250
300
350
N_2O ppbv
MkIV
OMS @ 615-637 K
ATMOS 3, 40°-50° N

Figure 11:

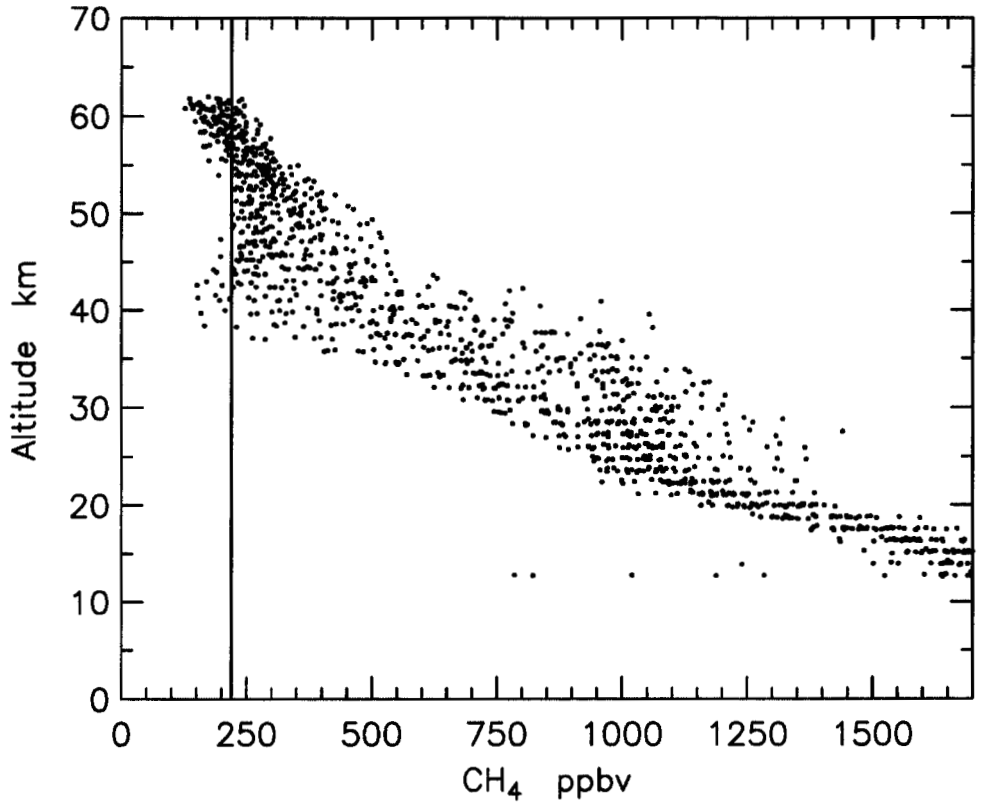
70
60
50
40
30
20
10
0
Altitude km
0
250
500
750
1000
1250
1500
CH4 ppbv

Figure 12:

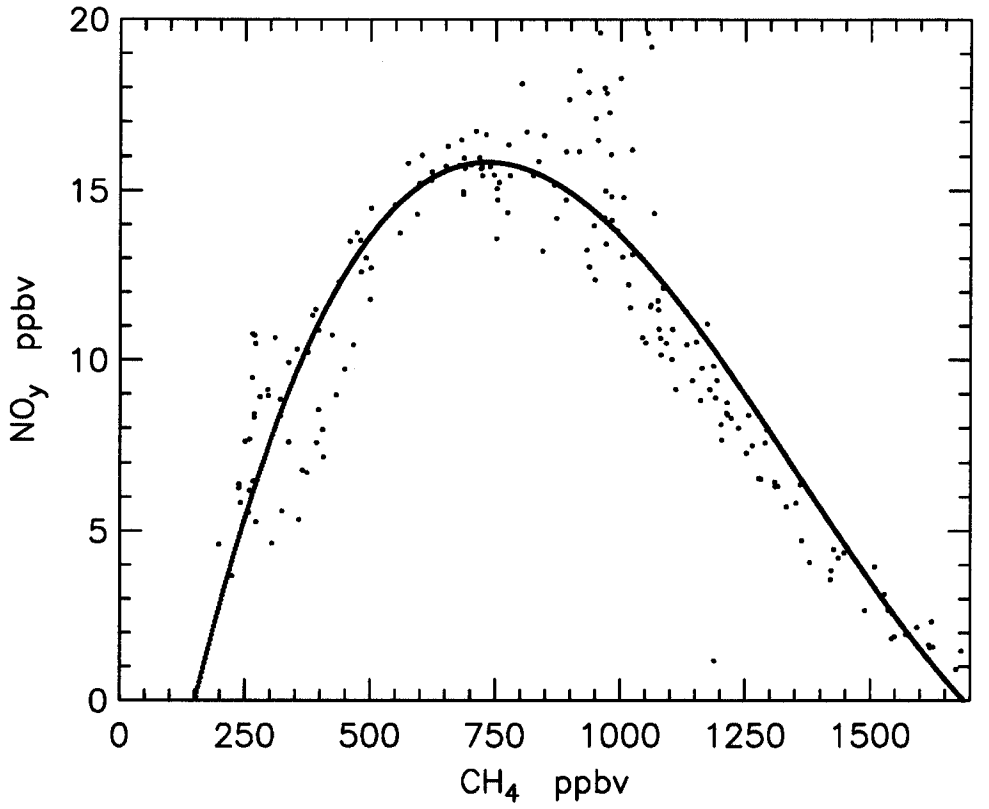

Figure 13:

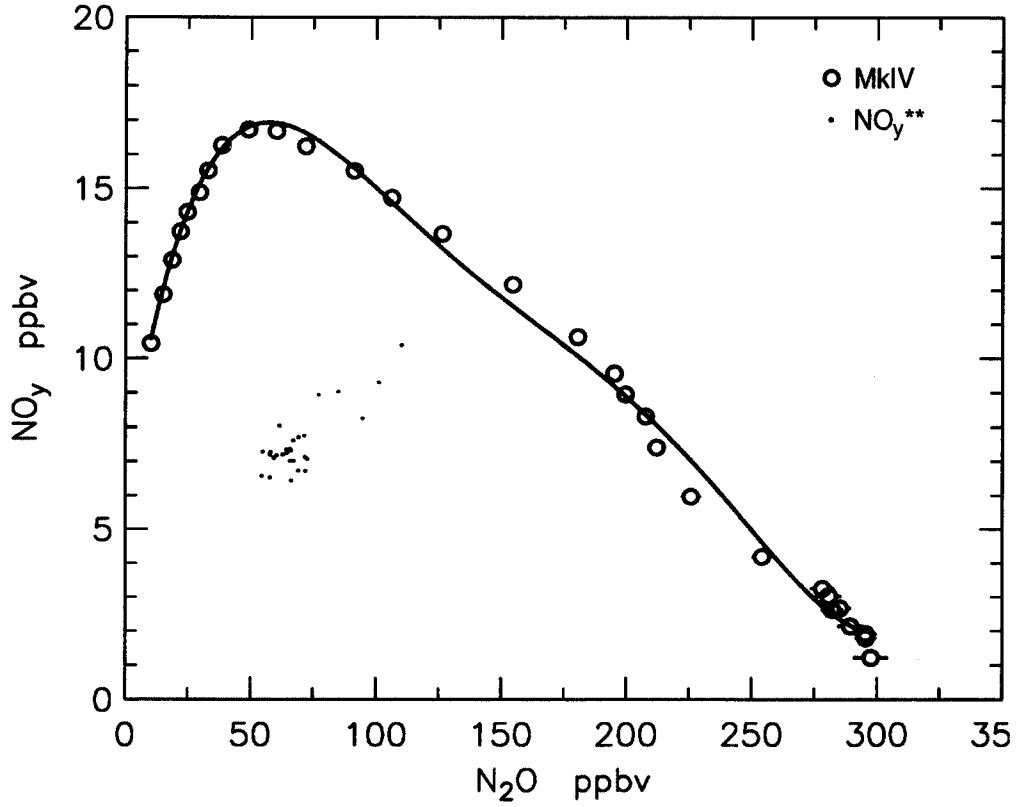

Figure 14: